Models and Methods for the Stability Assessment of Converters-dense DC Shipboard Microgrids

Andrea Alessia Tavagnutti
Dept. of Engineering and Architecture
University of Trieste
Trieste, Italy
andreaalessia.tavagnutti@dia.units.it

Massimiliano Chiandone
Dept. of Engineering and Architecture
University of Trieste
Trieste, Italy
mchiandone@units.it

Daniele Bosich
Dept. of Engineering and Architecture
University of Trieste
Trieste, Italy
dbosich@units.it

Giorgio Sulligoi
Dept. of Engineering and Architecture
University of Trieste
Trieste, Italy
gsulligoi@units.it

***Abstract*—In most advanced DC shipboard power systems, controlled power converters are conventionally adopted to ensure an efficient power flow from generating to load section. In these systems, a logical compromise between control targets (i.e. bandwidths) and power quality requirements (i.e. voltage/current ripples) is necessary to impose a stable dynamics behavior after perturbations. Although destabilizing interactions between controlled-filtered DC-DC converters are under-study since several years, an additional analytical development can help in better defining causes/solutions. This work wants to explore models and methods to analytically assess the voltage stability in converter-dense DC microgrids. The present paper is organized as a review, where each step-beyond to the final assessment moves from the reduced order modeling and the weighted bandwidth aggregation. Several examples and tools are proposed to clarify models limits and analytical methods' applicability.**

***Index Terms*—DC system, stability, WBM, analytical methods.**

I. Introduction

In the last years, the Medium Voltage Direct Current technology [1]-[3] is revolutionizing the shipboard electrical distribution [4]-[6]. By adopting a power converters-dense infrastructure, several are the promised advantages, among the most important flexibility in the power routing and resilience in presence of faults [7]-[9]. On the other hand, such a strong presence of controlled converters in an LC filtered system opens serious consequence on system stability after a perturbation [10]-[12]. Indeed, tight control bandwidths on the converters together with a no-standardized procedure in filtering design [13]-[16] can determine a low-damped, or even unstable system (i.e. system poles in right half plane) [17]-[19].

The present paper wants to propose a review on the models and methods to assess the system stability in DC shipboard microgrids. Most of the time, the discussed approach provides closed form analytical solutions, thus limiting the numerical calculations to specific cases having high-order equations.

II. Reduced Order Modeling

To reduce the complexity of the stability assessment process in a multi-converter DC systems, a possible alternative is to reduce, with appropriate assumptions, the order of the system. In particular, the filtering stage of the load side converter can be neglected for the purpose of the stability analysis. This assumption enables the aggregation of multiple loads, further simplifying the stability studies.

A. Stability Boundary of a Cascade Connected System

The order reduction hypothesis is verified on a cascade connected system, as the one in Fig.1, made up of a generating converter and a load one. The analytical stability boundaries of the complete cascade-connected system, Fig.1, and of the

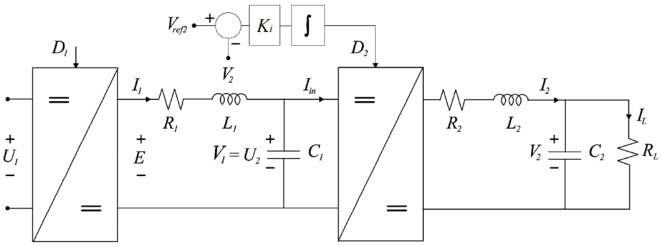

Fig. 1. Complete order cascade-connected DC power system [20].

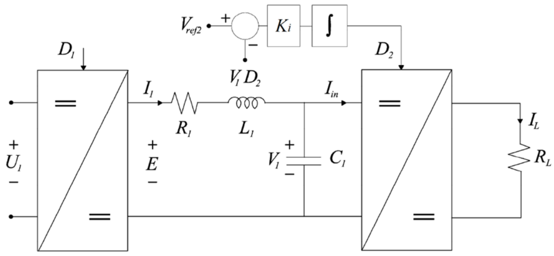

Fig. 2. Reduced-order cascade-connected DC power system [20].

979-8-3315-8138-1

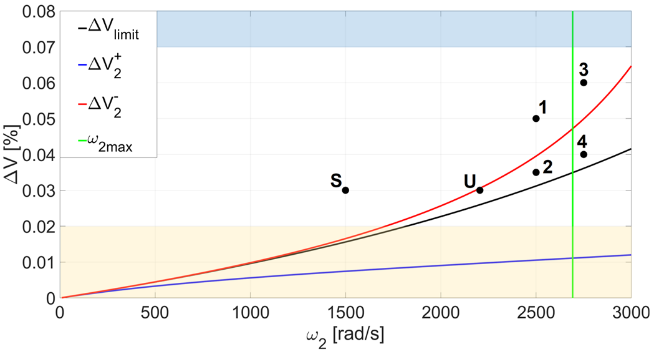

Fig. 3. Stability conditions on the ω_2-$\Delta V_{\%}$ plane [20].

the reduced one, Fig.2, are compared in [20]. In this analysis the generating converter is assumed as a ideal voltage source with its LC filtering stage, and for the load converter a simple integral regulator is used for the voltage control loop, while the inner current loop is considered as instantaneous. The input admittances of the load converter in Fig. 1 and Fig. 2 are as in eq. (1) and (2) respectively:

$$\overline{Y}_{in1} = \frac{\widetilde{I_{in}}}{\widetilde{V_1}} = \frac{D_{20}^2(R_L C_2 s^2 + s - \omega_2)}{L_2 C_2 R_L s^3 + L_2 s^2 + R_L s + R_L \omega_2} \quad (1)$$

$$\overline{Y}_{in1} = \frac{\widetilde{I_{in}}}{\widetilde{V_1}} = \frac{D_{20}^2(s - \omega_2)}{R_L(s + \omega_2)} \quad (2)$$

While the global admittance at the output of the generating converter for the two systems, $\overline{Y}_t$, can be found with eq. (3).

$$\frac{1}{\overline{Y_t}} = \overline{Z_t} = sL_1 + (sC_1 + \overline{Y_{in1}})^{-1} \quad (3)$$

To find the small-signal stability boundary of the systems, the eq. $DenY_t(s)=0$ has to be solved. While for the reduced order model the equation is easily solvable, as in (4), the problem is more complicated for the complete fifth order model. The solutions has however been found in [20] using an alternative formulation of the Routh-Hurwitz criterion. The stability boundaries for the fifth (red line) and third (green line) order models are in Fig. 3, as a function of the bus voltage ripple and of the load converter control bandwidth. The stable solutions for the third order model are all the ω_2-$\Delta V_{\%}$ combinations that are at the left of the green line, while for the fifth order model the stable area is represented by the ω_2-$\Delta V_{\%}$ combinations above the red line. By comparing the two curves and excluding the unfeasible regions (blue/yellow areas in Fig. 3) it is possible to visually identify the range of validity of the third order modeling hypothesis, thus defining its range of applicability.

$$\omega_{2max} = \frac{-L_1 D_2^2 + \sqrt{L_1^2 D_2^4 + 4R_L^2 L_1 C_1}}{2L_1 C_1 R_L} \quad (4)$$

B. Weighted Bandwidth Method

Such a method (WBM) aggregates a multitude of DC-DC controlled-load converters supplied from the same bus. It was proposed as resolutive in the study of complex radial-zonal shipboard power system with hundreds loads [21]. These step-down buck converters are responsible of controlling (i.e. first-order dynamics) the voltage on its own resistive load (i.e. modeling the demand from a shipboard area), while their LC filter is intentionally neglected to reduce the order of the entire system. This simplification is motivated when the control

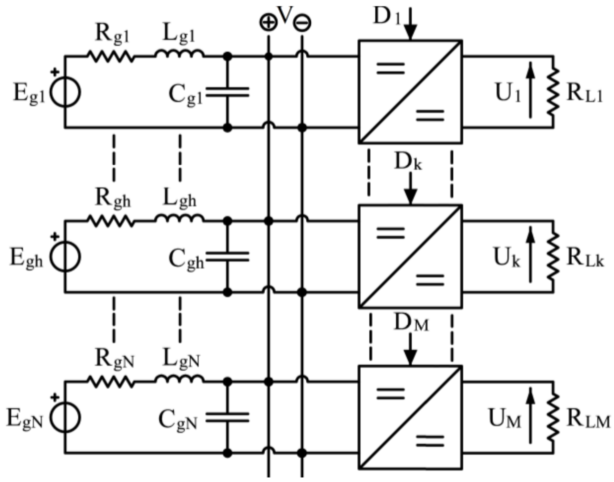

Fig. 4. Microgrid simplification under modeling assumptions [21].

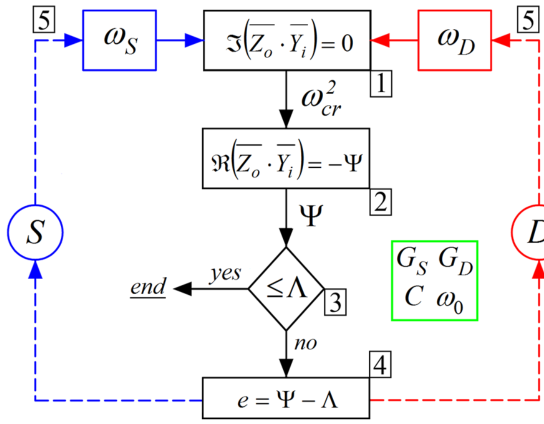

Fig. 5. Stability assessment iterative process [21].

$$\omega_B = \frac{-G_L + \sqrt{G_L^2 + 4C^2\omega_0^2}}{2C} \quad (5)$$

$$\begin{cases} P_L = \sum_{k=1}^{M} P_k = \sum_{k=1}^{Ms} P_k + \sum_{k=Ms+1}^{M} P_k = P_S + P_D \\ G_L = \sum_{k=1}^{M} G_k = \sum_{k=1}^{Ms} G_k + \sum_{k=Ms+1}^{M} G_k = G_S + G_D \end{cases} \quad (6)$$

$$\begin{cases} \omega_S = \sum_{k=1}^{Ms} m_k \omega_k & (7a) \\ \omega_D = \sum_{k=Ms+1}^{M} m_k \omega_k & (7b) \end{cases}$$

$$\begin{cases} \Im(\overline{Z_o} \cdot \overline{Y_i}) = -\frac{\omega_{cr}}{C(\omega_0^2 - \omega_{cr}^2)} \cdot \left[G_S \frac{\omega_S^2 - \omega_{cr}^2}{\omega_S^2 + \omega_{cr}^2} + G_D \frac{\omega_D^2 - \omega_{cr}^2}{\omega_D^2 + \omega_{cr}^2} \right] = 0 & (8a) \\ \Re(\overline{Z_o} \cdot \overline{Y_i}) = -\frac{2\omega_{cr}^2}{C(\omega_0^2 - \omega_{cr}^2)} \cdot \left[G_S \frac{\omega_S}{\omega_S^2 + \omega_{cr}^2} + G_D \frac{\omega_D}{\omega_D^2 + \omega_{cr}^2} \right] = -\Psi & (8b) \end{cases}$$

bandwidth is sufficiently smaller than then the related filter resonance frequency. By hypothesizing a large distance in bandwidth between load section's converters (e.g. 20-1500 rad/s) and generating part at steady state, the entire system can be modeled as in Fig. 4 for what regard the DC stability assessment. Then, the load aggregation based on the (5) splitter is used to group low-bandwidth controlled loads (i.e. $\omega_k < \omega_B$) as a single stabilizing load having G_S (6) conductance. Differently, high dynamics loads (i.e. $\omega_k > \omega_B$) are forming a single G_D conductance. The two aggregated loads are respectively controlled by ω_S (i.e. stabilizing bandwidth) and ω_D (i.e. destabilizing bandwidth), whose definitions are expressed in (7). Here, the conductance ratios m_k are obtained by dividing the single conductance G_k by the total stabilizing/destabilizing conductance (i.e. G_S or G_D basing on the load dynamics characteristic). The resulting ω_S and ω_D are a sort of center of gravity, both capable of aggregating the stabilizing/destabilizing nature of the modeled controlled converters. When the loads multitude is joined in two loads (i.e. ω_S,G_S and ω_D,G_D), the iterative procedure in Fig. 5 is adopted to define the minimum equivalent stabilizing quota to balance the destabilizing one thus ensuring a specified negative-stable intersection (i.e. -Λ, where Λ<1) on the Gauss plane (i.e. Nyquist stability criterion) [22]. This iterative process exploits equation (8a) and (8b) to define step-by-step the intersection on real-axis, thus guaranteeing the related stable position. By assuming the generating part at steady state and the presence of destabilizing converters, the WBM analytical approach plus the numerical-iterative process (Fig. 5) can conveniently identify the stabilizing power/bandwidth quota for assuring the DC system stability. Additional activity can also envisage the control bandwidths on generating converters, thus increasing the order in differential equations. A third path of development may introduce also boost converters functionality or current control mode to extend the WBM applicability.

III. Weighted Bandwidth Method Applications

The WBM makes it possible to group the loads of a complex multi-converter power system into two aggregated sets. By simplifying stability evaluation, this aggregation is suitable for the preliminary design of power systems and for integration into Power Management Systems (PMSs). In particular, incorporating stability assessment capabilities into the PMS increases overall system reliability and enables the implementation of safe reconfiguration strategies within the system controller. The reconfiguration process may be performed manually, using the stability evaluations as decision support [23], or it can be fully automated if an optimization framework is embedded in the controller [24]-[25]. Therefore, the WBM can be used to define stability maps, thus the best-stable combination among stabilizing/destabilizing converters.

A. Stability Maps

Considering a power system with M loads, as in Fig. 4, the loads can be divided into two sets (stabilizing and destabilizing) using the WBM. By applying the iterative process described in Fig. 5, it is possible to determine, for each combination of $\omega_D - m_D$, the corresponding maximum ω_s that ensures system stability. This procedure yields a 3D stability map, such as the one in Fig. 6. The map can be intersected at a given m_D to obtain 2D stability maps, as in Fig. 7. In the 2D maps, the stable operating region for a given m_D is represented by the $\omega_S - \omega_D$ pairs below the corresponding boundary curve. If the PMS is equipped with these stability maps, it can verify system stability prior to any load or configuration change, ensuring that the operating point remains within the stable region. An example is provided in Fig. 8, where a transition across three operating points is shown, all of which remain within the stable region.

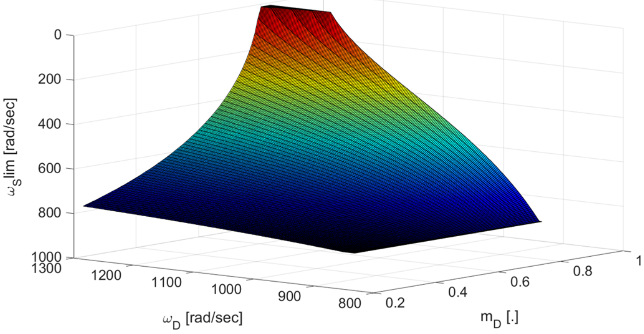

Fig. 6. 3D stability map, P_L=24 MW and ω_B=832 rad/s [23].

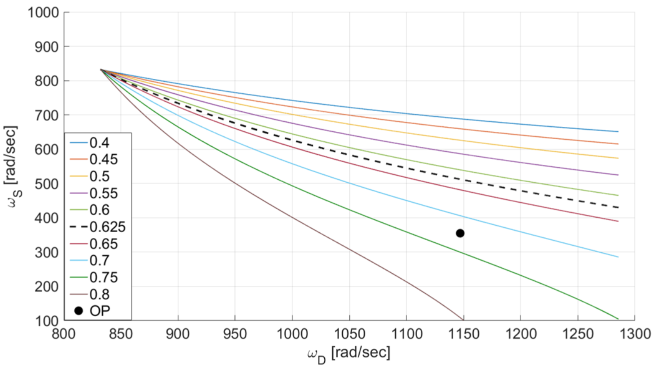

Fig. 7. 2D stability map, P_L=24 MW and ω_B=832 rad/s [23].

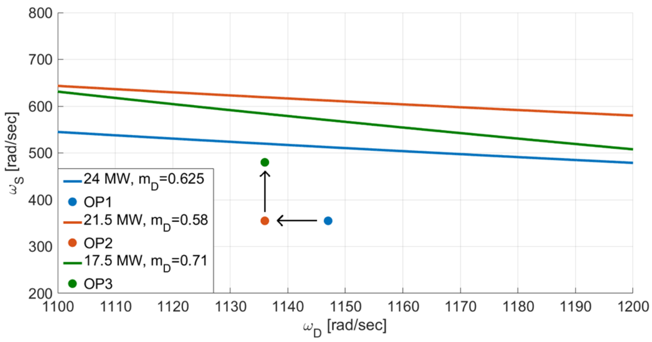

Fig. 8. Operating points transition on 2D stability map [23].

B. Optimized Reconfiguration

While the stability maps introduced in [23] can be an effective tool to perform the stability assessment online, they require a set of rules or a decision-making algorithm in order to be used as an active reconfiguration tool. In [23], the decision making process is assigned to a human operator, whereas in [24] and [25] the PMS has been equipped with an optimization algorithm, eq. (9)-(10). When a load or configuration change is requested, the controller first evaluates the stability of the resulting operating point before any physical modification is applied to the system. If the new operating condition lies within the unstable region, the optimization algorithm reduces the control bandwidth of the stabilizing loads to obtain an equivalent control bandwidth ω_{obj}. The achievement of a target control bandwidth is enforced as a constraint, eq. (10), while the objective function seeks to minimize the deviation of the stabilizing control bandwidths from their rated ones, eq. (9). A

$$\min f(\omega_{Si}) = \sum_{i=1}^{8}(\overline{\omega_{Si}} - \omega_{Si})^2 \quad (9)$$

$$\frac{\sum_{i=1}^{8} P_1\omega_1}{P_S} = \omega_{Sobj} \quad (3) \qquad \sum_{i=1}^{8} \omega_{Si} \in [\omega_{Simin}, \omega_{Simax}] \quad (10)$$

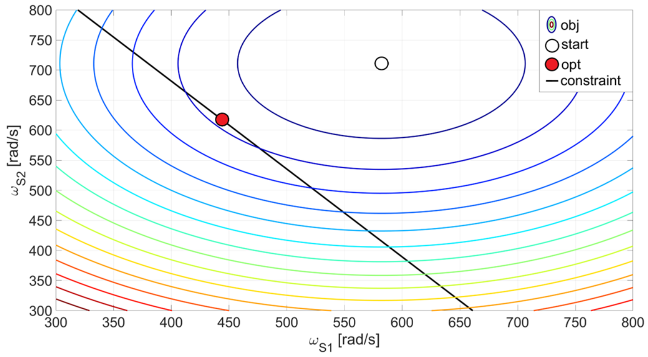

Fig. 9. Objective function contours [24].

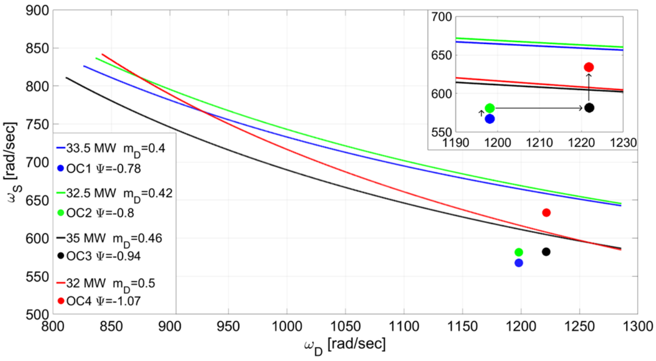

Fig. 10. Operating condition evolution during the unstable test [25].

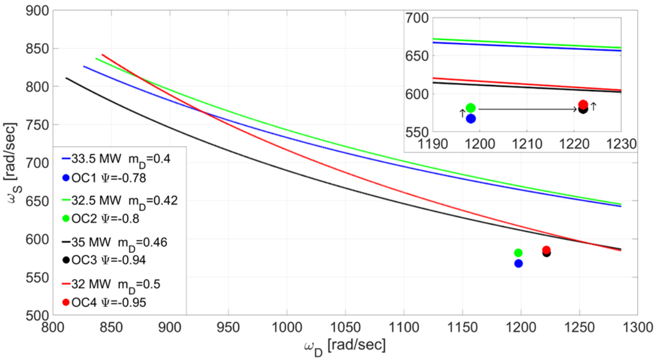

Fig. 11. Operating conditions evolution during the stable test [25].

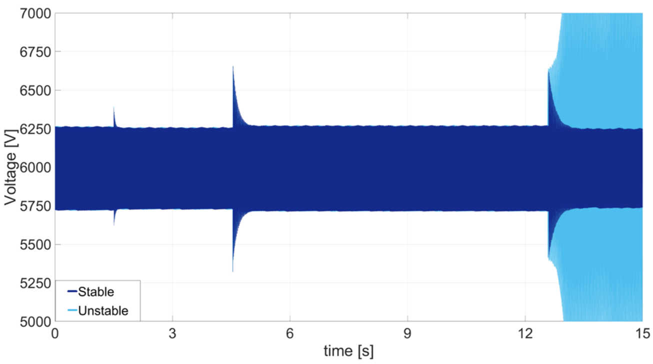

Fig. 12. Bus voltage transients (cyan unstable, blue stable) [25].

visual representation of the optimization process in given in Fig. 9 where a example case study with only two stabilizing converter is used as a reference. The use of the stability maps in combination with the optimization-based reconfiguration strategy is illustrated in Fig. 10 and Fig. 11. These figures show the transition between operating points, from an initial condition (blue marker) to a final one (red marker). In Fig. 10, the final operating condition lies within the unstable region, therefore, a reconfiguration is required to maintain system stability after the load change. The optimization algorithm performs this reconfiguration automatically, prior to any physical modification of the system. This effect is shown in Fig. 11, where the final operating point is shifted into the stable region due to the reduction of the control bandwidths of the stabilizing loads. To validate the analytical considerations, the proposed algorithm is tested using a CHIL configuration. The power system is accurately modeled on a Typhoon HIL 604 platform, while the converter power setpoints and control bandwidth adjustments are issued from an external PC on which the PMS is implemented. Fig. 12 shows the voltage transient on the main DC bus during the operating point transitions. At each transition, the voltage exhibits a transient response before settling to a new equilibrium. The only exception occurs during the final transition: without reconfiguration capability, the system enters an unstable evolution (cyan trace), whereas PMS with stable reconfiguration functionality maintains a stable-dark response.

C. *Simplified analytical approach*

By assuming a global radial model where controlled load converters are grouped in stabilizing-destabilizing aggregates, the analysis in [26] ensures an analytical-simplified approach in the definition of the stability margin. From a first complete analysis by complex iterative-numerical loops, a simplified-conservative method [26] provides a smaller limit bandwidth on stabilizing converter (thus more effective in compensating for the ω_D unstable behavior). The simplified approach is considered a good method to quickly define the stability limits. If the iterative approach provides the stabilizing control bandwidth to perfectly compensate for the destabilizing effect, as a matter of fact the analytical value certainly ensures a stability margin, while at the same time improving the algorithm time-efficiency.

IV. Generating Converters

Previous considerations have identified the stability limits in a DC controlled system, while assuming a steady-state output impedance. This strong assumption is true when the control bandwidths on the generating part are substantially (100x) smaller than the bandwidths on the load section. Conversely, when bandwidths are comparable also the control on the generating converters impacts on the global stability.

A. *Nyquist stability analysis*

The Nyquist criterion [22] is a method to evaluate the DC system stability by only observing the product $Zo(j\omega)Yi(j\omega)$ while increasing the frequency ω. By observing this curve on Gauss plane, the system stability is certainly proved when the curve does not clockwise-encircle the point (-1,0). A consequent criterion mostly adopted in industry prefers to determine the stability by only verifying if $\Re[Zo{\cdot}Yi]$>-1 when

$\Im[Zo \cdot Yi]=0$. If the multitude of controlled loads can be aggregated by the WBM for Nyquist test, different approach when modeling the generating impedance.

B. Generating Converters Aggregation

For adopting the Nyquist stability criterion [22], both output impedance and input admittance are to be defined. The single input admittance (i.e. voltage-controlled DC-DC buck) is provided in (1)-(2), while the aggregation of several can follow the WBM. For what regards the output impedance, a different modeling is necessary. For the initial case of single impedance [27], two filtered DC-DC step-down converters on the same bus are aggregated as in (11). Then, increasing one converter on the generating part determines the impedance (12). Finally, the case shown in (13) constitutes the general expression for modelling *N* filtered converters on the same bus.

$$\overline{Z_0}(s) = \frac{V(s)}{-I_L(s)} = \frac{s^2 L_1 L_2}{s^3(L_1 L_2 C)+s(L_1+L_2)+\omega_1 L_2+\omega_2 L_1} \tag{11}$$

$$\overline{Z_0}(s) = \frac{s^2 L_1 L_2 L_3}{s^3(L_1 L_2 L_3 C)+s(L_1 L_2+L_2 L_3+L_1)+\omega_1 L_2 L_3+\omega_2 L_1 L_3+\omega_3 L_1 L_2} \tag{12}$$

$$\overline{Z_0}(s) = \frac{s^2 \prod_{k=1}^{N} L_k}{s^3 C \prod_{k=1}^{N} L_k + s\sum_{k=1}^{N} L_k \prod_{j=k+1}^{N} L_j + \sum_{k=1}^{N} \omega_k \prod_{j=k+1}^{N} L_j} \tag{13}$$

V. CONCLUSIONS

The present work has provided a review on models and methods to analyze the voltage stability in complex DC shipboard power grids. From an initial order reduction on a cascaded-converters case, the paper has introduced the Weighted Bandwidth Method as resolutive in the stability analysis of converters-dense systems. Then, the WBM is applied to calibrate the Power Management Systems. Finally, the Nyquist criterion is confirmed as resolutive in stability assessment, while an impedance aggregation is introduced for the modeling of the controlled generating systems.

ACKNOWLEDGMENT

The authors wish to thank Prof. Giovanni Giadrossi for his valuable contribution. The authors would like to thank Typhoon HIL for providing the HIL platform used in the development of this research work.

REFERENCES

[1] M.M.S. Khan et al., "Fuzzy Logic Based Energy Storage Management System for MVDC Power System of All Electric Ship," in *IEEE Tran. on Energy Conv*., vol.32, no.2, pp.798-809, June 2017.

[2] B. Zhao et al., "Modular Multilevel High-Frequency-Link DC Transformer Based on Dual Active Phase-Shift Principle for Medium-Voltage DC Power Distribution Application," in *IEEE Transactions on Power Electronics*, vol. 32, no. 3, pp. 1779-1791, March 2017.

[3] G. Ning et al., "Single-Stage IIOS Converter With Auto-Voltage-Sharing for Distributed Photovoltaic MVDC Collection System," in *IEEE Trans. on Power Electronics*, vol. 39, no. 11, pp. 14172-14178, Nov. 2024.

[4] A. Latorre et al., "Shipboard DC Systems—A Critical Overview: Challenges in Primary Distribution, Power-Electronics-Based Protection, and Power Scalability," in *IEEE Open Jour. of the Ind. Elec. Society*, vol. 4, pp. 259-286, 2023.

[5] J. Khazaei, "Optimal Flow of MVDC Shipboard Microgrids With Hybrid Storage Enhanced With Capacitive and Resistive Droop Controllers," in *IEEE Trans. on Power Systems*, vol. 36, no. 4, pp. 3728-3739, July 2021.

[6] S. Faddel, A. A. Saad, T. Youssef and O. Mohammed, "Decentralized Control Algorithm for the Hybrid Energy Storage of Shipboard Power System," in *IEEE Journal of Emerging and Selected Topics in Power Electronics*, vol. 8, no. 1, pp. 720-731, March 2020.

[7] M. Andrus, H. Ravindra, J. Hauer, M. Steurer, M. Bosworth and R. Soman, "PHIL implementation of a MVDC fault management test bed for ship power systems based on megawatt-scale modular multilevel converters," *2015 IEEE Electric Ship Technologies Symposium (ESTS)*, Old Town Alexandria, VA, USA, 2015.

[8] A. Kwasinski, "Advanced power electronics enabled distribution architectures: Design, operation, and control," *ECCE Asia*, Jeju, Korea (South), 2011, pp. 1484-1491.

[9] H. Mahdi, B. Hoff and T. Østrem, "A Review of Power Converters for Ships Electrification," in *IEEE Transactions on Power Electronics*, vol. 38, no. 4, pp. 4680-4697, April 2023.

[10] Y. Li, J. Li, H. Xiao, J. Zhang and Z. Du, "Stability Analysis of Droop-Based Converter Using SISO Method From DC Side Perturbation," in *IEEE Trans. on Power Delivery*, vol. 36, no. 5, pp. 3150-3161, Oct. 2021.

[11] Y. Chen et al., "Stability Analysis and Impedance Reshaping Methods for DC Distribution Systems with Multiple Voltage Sources," *2024 IEEE CIEEC*, Harbin, China, 2024, pp. 1720-1725.

[12] N. Hatziargyriou et al., "Definition and Classification of Power System Stability – Revisited & Extended," in *IEEE Transactions on Power Systems*, vol. 36, no. 4, pp. 3271-3281, July 2021.

[13] L. Xu et al., "A Review of DC Shipboard Microgrids—Part II: Control Architectures, Stability Analysis, and Protection Schemes," in *IEEE Trans. on Power Electronics*, vol. 37, no. 4, pp. 4105-4120, April 2022.

[14] S. Chevalier, F. M. Ibanez, K. Cavanagh, K. Turitsyn, L. Daniel and P. Vorobev, "Network Topology Invariant Stability Certificates for DC Microgrids With Arbitrary Load Dynamics," in *IEEE Transactions on Power Systems*, vol. 37, no. 3, pp. 1782-1797, May 2022.

[15] B. He et al., "A Power Adaptive Impedance Reshaping Strategy for Cascaded DC System With Buck-Type Constant Power Load," in *IEEE Trans. on Power Electronics*, vol. 37, no. 8, pp. 8909-8920, Aug. 2022.

[16] K. A. Potty, E. Bauer, H. Li and J. Wang, "Smart Resistor: Stabilization of DC Microgrids Containing Constant Power Loads Using High-Bandwidth Power Converters and Energy Storage," in *IEEE Trans. on Power Electronics*, vol. 35, no. 1, pp. 957-967, Jan. 2020.

[17] J. Li et al., "Impedance-Based Instability Participation Analysis for DC Distribution Systems," *2024 7th CEEPE*, Yangzhou, China, 2024.

[18] T. Fang et al., "Analysis and Suppression Method of High-Frequency Oscillation in Parallel DC-DC Converter System," *2025 AEEES*, Chengdu, China, 2025, pp. 216-221.

[19] L. Fan and Z. Miao, "Admittance-Based Stability Analysis: Bode Plots, Nyquist Diagrams or Eigenvalue Analysis?," in *IEEE Transactions on Power Systems*, vol. 35, no. 4, pp. 3312-3315, July 2020.

[20] A.A. Tavagnutti, D. Bosich, S. Pastore and G. Sulligoi, "A Reduced Order Model for the Stable LC-Filter Design on Shipboard DC Microgrids," *2023 IEEE ESARS-ITEC*, Venice, Italy, 2023, pp. 1-6.

[21] D. Bosich, et al., "Weighted Bandwidth Method for Stability Assessment of Complex DC Power Systems on Ships", *Energies 2022*, 15, 258.

[22] X. Feng, Z. Ye, K. Xing, F. Lee, D. Borojevic, "Individual load impedance specification for a stable DC distributed power system", in *Proceedings of the APEC'99*, Dallas, TX, USA, 14–18 March 1999.

[23] A.A. Tavagnutti, D. Bosich and G. Sulligoi, "The WBM Reconfiguration to Prevent the Instability on DC Shipboard Microgrids," *2022 SEST*, Eindhoven, Netherlands, 2022, pp. 1-6.

[24] A. A. Tavagnutti, D. Bosich and G. Sulligoi, "Optimized Tuning for Flexible and Resilient Control of Zonal DC Microgrids on Ships," *2023 IEEE PESGM 2023*, Orlando, FL, USA, 2023, pp. 1-5.

[25] A. A. Tavagnutti, M. Chiandone, D. Bosich and G. Sulligoi, "A Stability-Aimed PMS for Shipboard Zonal DC Microgrids: The C-HIL Tests on Real-Time Platform," *2023 IEEE Electric Ship Technologies Symposium (ESTS)*, Alexandria, VA, USA, 2023, pp. 453-457.

[26] A. A. Tavagnutti, D. Bosich and G. Sulligoi, "Analytical Approach to Define the Stability Boundaries in Controlled DC Microgrids," *2024 IEEE ESARS-ITEC 2024*, Naples, Italy, 2024, pp. 1-6.

[27] A. A. Tavagnutti, D. Bosich, M. D. Feste and G. Sulligoi, "On the Modeling of DC-DC Converters for Stability Assessment of DC Zeds on Ships," *2025 IEEE Electric Ship Technologies Symposium (ESTS)*, Alexandria, VA, USA, 2025, pp. 291-298.

979-8-3315-8138-1